Tribochemistry and material transfer for the ultrananocrystalline diamond-silicon nitride interface revealed by x-ray photoelectron emission spectromicroscopy

David S. Grierson and Anirudha V. Sumant[a)]
Engineering Physics Department, University of Wisconsin-Madison, Wisconsin 53706

Andrew R. Konicek
Physics Department, University of Wisconsin-Madison, Wisconsin 53706-1390

Mike Abrecht
Synchrotron Radiation Center, Stoughton, Wisconsin 53589-3097

J. Birrell, Orlando Auciello, and John A. Carlisle[b)]
Materials Science Division and Center for Nanoscale Materials, Argonne National Laboratory, Argonne, Illinois 60439

Thomas W. Scharf[c)] and Michael T. Dugger
Sandia National Laboratories, Albuquerque, New Mexico

P. U. P. A. Gilbert[d)]
Physics Department, University of Wisconsin-Madison, Wisconsin 53706-1390

Robert W. Carpick[e)]
Engineering Physics Department, University of Wisconsin-Madison, Wisconsin 53706

(Received 18 May 2006; accepted 20 August 2007; published 19 September 2007)

The authors report tribochemical changes due to sliding of a silicon nitride (Si_3N_4) ball against an ultrananocrystalline diamond (UNCD) thin film. Unidirectional sliding wear measurements were conducted for 2000 cycles using a ball-on-disk apparatus with a 3/16 in. diameter Si_3N_4 ball at a sliding speed of 3.3 mm/s and a normal load of 98.0 mN (nominal Hertzian stress of 0.6 GPa) in a nitrogen environment at 50% relative humidity at room temperature. The wear track produced on the UNCD film was analyzed by X-ray photoelectron emission spectromicroscopy (X-PEEM) combined with X-ray absorption near-edge structure (XANES) spectroscopy to identify and spatially resolve chemical changes inside the wear track, particularly rehybridization of carbon. XANES spectra show that SiO_x complexes are deposited within the wear track. Very little rehybridization of the UNCD from its primarily sp^3 bonding configuration to sp^2 bonding is observed, and there is no observable oxidation of the UNCD, pointing to the impressive stability of the film under significant tribological loading conditions. Raman spectroscopy of the worn portion of the Si_3N_4 ball shows that disordered carbon is found on the worn surface. The authors attribute the formation of SiO_x complexes within the wear track to wear of the ball and subsequent deposition into the track. The authors attribute the disordered carbon on the Si_3N_4 ball to removal of sp^2-bonded carbon from the UNCD surface and subsequent accumulation onto the ball's surface. This work demonstrates the potential of X-PEEM for the study of tribochemical modifications of carbon-based thin film surfaces. © *2007 American Vacuum Society.* [DOI: 10.1116/1.2782428]

I. INTRODUCTION

There is a scientific and technological need to develop a fundamental understanding of material transfer and tribochemical reactions between rolling and/or sliding surfaces at the microscale/nanoscale. Understanding tribochemical reactions at these scales is needed to engineer reliable moving mechanical assemblies, such as micromechanical systems (MEMS)/nanoelectromechanical systems (NEMS) involving components that contact and slide. The development of physical models to represent tribological interactions requires insightful experimental data from advanced surface characterization techniques. As well, the development of reliable MEMS/NEMS systems with contacting parts requires advanced materials with superior mechanical and tribological properties.

The characterization of tribochemical phases induced by sliding and third body tribology is the focus of a large body of work in the literature.[1–4] These studies involve both *in situ* and *ex situ* techniques to analyze surfaces during and after sliding. The goal of these investigations is to characterize

[a)]Present address: Center for Nanoscale Materials, Argonne National Laboratory, Argonne, IL.
[b)]Present address: Advanced Diamond Technologies, Romeoville, IL.
[c)]Present address: University of North Texas, Department of Materials Science and Engineering, Denton, TX.
[d)]Previously publishing as Gelsomina De Stasio.
[e)]Present address: University of Pennsylvania, Department of Mechanical Engineering and Applied Mechanics, Philadelphia, PA.

tribological systems to understand how material properties, sliding conditions, and modifications induced by sliding affect adhesion, friction, and wear. Identification of the compositions and phases of transfer films formed in various material systems has allowed several mechanisms by which these films lower friction and wear to be proposed. For solid lubricants, it has been repeatedly shown that third bodies and tribochemical reactions are crucial in determining the tribological performance. However, a predictive model that fully describes the behavior of tribological systems does not exist. Therefore, there is still a need to develop such models of friction and wear, particularly for novel materials with tribological properties that have potential for emerging applications such as MEMS/NEMS.

The exceptional mechanical and tribological properties of diamond[5] make it a promising structural material for MEMS/NEMS and other applications. Ultrananocrystalline diamond (UNCD), a nanostructured diamond material in thin film form developed at Argonne National Laboratory, is comprised of phase-pure diamond grains and atomically abrupt grain boundaries, with up to 98% sp^3 bonding overall.[6] The residual sp^2 bonding is entirely attributed to grain boundaries. UNCD films, synthesized using an argon-rich Ar (99%)/CH_4 (1%) gas chemistry in a microwave plasma enhanced chemical vapor deposition system, have equiaxed grains with diameters in the range of 2–5 nm, atomically abrupt (0.4 nm) grain boundaries, and smooth surfaces as-deposited (RMS roughness <10 nm over a 1×1 μm^2 area).[7] Mechanical property measurements show that the modulus, hardness, and fracture properties approach those of single crystal diamond.[8–10] Surface micromachined MEMS structures can be fabricated from UNCD.[11]

X-ray photoelectron emission spectromicroscopy (X-PEEM) combined with X-ray absorption near-edge structure (XANES) spectroscopy are powerful tools for studying chemical bonding structure at high spatial resolution (down to 10 nm).[12] X-PEEM yields local information about the chemical composition and bonding of the atoms at the surface (top ~3 nm at the carbon *K* edge) of a sample[13] and is particularly sensitive to the hybridization state of carbon. For tribological studies, X-PEEM can resolve micro/nanotribochemistry of a sample, as XANES spectra can be extracted from selected regions inside and outside of a wear track, allowing direct comparison of tribologically modified and unmodified regions.[14–18] To demonstrate this potential, we studied a wear track formed on the surface of an UNCD film by a silicon nitride (Si_3N_4) ball using X-PEEM. The worn area of the Si_3N_4 ball was characterized by Raman spectroscopy. The results demonstrate the power of X-PEEM analysis to resolve subtle chemical changes on the surface of UNCD inside the wear track.

II. EXPERIMENTAL METHODOLOGY

Friction measurements were made using a ball-on-disk linear wear tester on the surface of a planar UNCD film deposited onto a silicon substrate. The tests were performed in a unidirectional sliding mode. The tester was housed in an environmental chamber. Oxygen content in the chamber was measured using a Delta F Platinum Series oxygen monitor, and the dew point was monitored with a chilled mirror hygrometer. Tests were conducted at 50% RH in nitrogen, with <20 ppm O_2, using a 3/16 in. diameter Si_3N_4 ball with arithmetic surface roughness R_a of 3 nm, at a normal load of 98.0 mN. This load corresponds to an initial maximum Hertzian contact stress of ~0.6 GPa. A 500 mN transducer (Sensotec) in the load arm measured the tangential load over a track distance of 1.6 mm, with a sliding speed of 3.3 mm/s. The ratio of tangential to normal load is the reported friction coefficient. At least five friction tests were run for 2000 unidirectional cycles, and one of the wear tracks produced from this series of tests is analyzed thoroughly in this article.

Shortly after sliding, micro-Raman spectra were obtained on the Si_3N_4 ball surface using a 514 nm argon laser excitation at a low power of 20 mW. The laser beam was focused to a ~1 μm spot size. At this laser power density (~25 mW/μm^2), no changes in the spectra due to surface heating were expected or observed. The acquisition times were 60 s/spectrum with 5 total accumulations taken to average each spectrum. Raman shifts were measured over a frequency range from 200 to 1800 cm^{-1}, with 1 cm^{-1} resolution.

All X-PEEM work was performed several months after the wear tracks had been produced. The sample was stored in dry nitrogen in the interim. X-PEEM was performed *ex situ* using the spectromicroscope for the photoelectron imaging of nanostructures with X-rays (SPHINX) instrument[12] at the Synchrotron Radiation Center (SRC), University of Wisconsin-Madison. Immediately before SPHINX analysis, the sample was sputter coated with 1 nm of Pt in the area of analysis and 50 nm of Pt around it to improve conductivity.[13] The 1 nm Pt coating is well below the photoelectron escape depth of ~3 nm at the C, Si, and O *K* edges that we selected[13] and thus does not inhibit our measurements. The samples were then inserted into the PEEM vacuum system within 30 min and analyzed in ultrahigh vacuum (10^{-9} Torr). All XANES spectra were first normalized by ratio to a beam line background curve simultaneously acquired on the region covered with 50 nm of Pt, which essentially provides a C-, Si-, and O-free reference. Subsequently, all C 1*s* spectra were normalized again to set the pre- and post-edge regions (at 280.0 and 310.0 eV, respectively) of the spectrum to intensities zero and one, respectively. Normalization to the beamline background acquired on Pt eliminates the effects of carbon contamination within the beamline optics, and setting the post-edge intensity to one allows for quantitative comparison of the relative peak intensities from different spectra.

III. RESULTS AND DISCUSSION

Figure 1 shows the variation in friction coefficient between a Si_3N_4 ball and UNCD over the course of 2000 unidirectional sliding cycles. After a run-in period of ~500 cycles, the friction coefficient reached a steady-state average value of ~0.2. This value of 0.2 is significantly higher than coefficients of friction reported elsewhere for

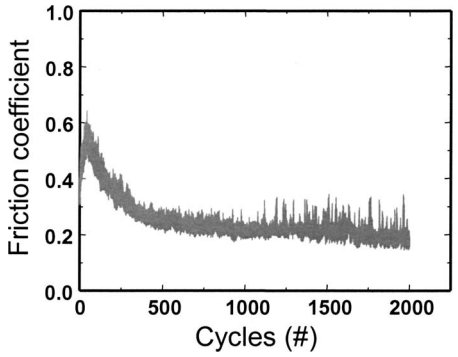

FIG. 1. Friction coefficient of Si_3N_4 on UNCD as a function of number of cycles.

UNCD films. Previous tribological studies of UNCD films run against Si_3N_4 counterfaces gave friction coefficient values ranging from 0.04 to 0.1 depending upon the testing environment (i.e., humid air versus dry N_2).[19,20] The sliding velocity used in the present case (3.3 mm/s) is ~15 times lower than that used previously (50 mm/s), and the nominal Hertzian stress is ~0.6 times lower, both of which may account for the higher friction coefficient observed in our experiment.[19,20]

To analyze the chemical changes induced by wear, C 1*s*, O 1*s*, and Si 2*p* XANES spectra were extracted from specific regions of the worn and unworn UNCD sample imaged in the PEEM instrument. A PEEM image taken at 310.0 eV [Fig. 2(a)] and a Si–O, O $1s \rightarrow \sigma^*$ division map [Fig. 2(b)] are displayed along with a series of C 1*s* XANES spectra [Fig. 2(c)]. The 310.0 eV image simply provides contrast within the energy region of carbon absorption, which allows us to identify the wear track. The vertical striations observed through the center of the X-PEEM image are the wear marks induced from the wear test and can arise from both topographic and chemical differences. The Si–O, O $1s \rightarrow \sigma^*$ division map was obtained by dividing the intensity of each pixel in a PEEM image taken at 538.0 eV (which is within the O $1s \rightarrow \sigma^*$ transition region for Si–O bonds, as identified by correlating the O 1*s* spectra with the Si *L*-edge spectra discussed later) by the intensity from corresponding pixels in a PEEM image taken at 530.0 eV (which is below the O 1*s* absorption edge). This division map thus provides contrast associated with variations in the concentration of Si–O bonds, with darker regions corresponding to regions of higher Si–O bond concentration. The division map was then used to select ten regions inside the wear track, with regions 1–5 corresponding to areas with a higher concentration of oxygen, and regions 6–10 corresponding to regions with a lower concentration of oxygen.

Overall, the chemical differences between regions 1–5 and regions 6–10 are attributed to the nonuniform way in which the contact pressure was distributed within the contact zone, leading to different tribochemistry and/or material transfer, discussed further below. The plotted spectra in Fig. 2(c) are extracted from areas 1–10 and from one additional area outside of the wear track (five regions outside the track

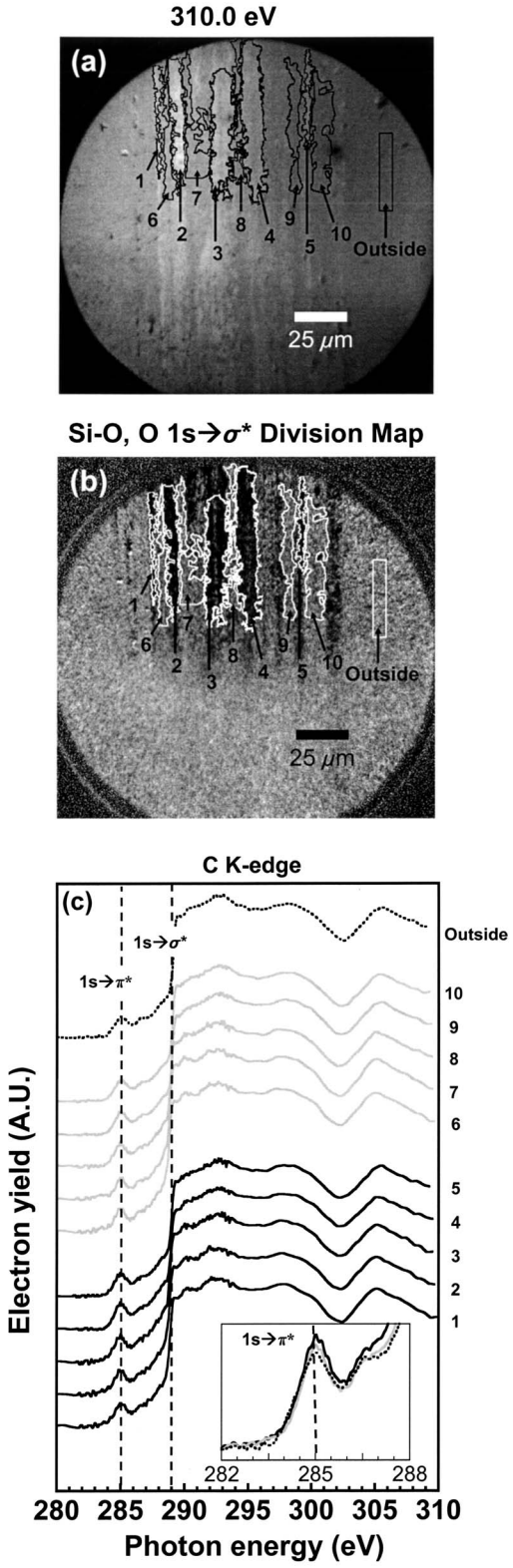

FIG. 2. (a) PEEM image of the wear track taken with 310.0 eV X-rays illuminating the sample. (b) Si–O, $1s \rightarrow \sigma^*$ division map. Darker regions in the division map correspond to a higher concentration of Si–O bonds. (c) C 1*s* XANES spectra obtained from the regions outlined in (a) and (b). The transition to the π^* orbitals of unsaturated carbon-carbon bonds ($1s \rightarrow \pi^*$), and the onset of transitions to σ^* orbitals in carbon-carbon bonds ($1s \rightarrow \sigma^*$), are indicated. The inset to (c) shows three average spectra of the C $1s \rightarrow \pi^*$ peak region obtained by averaging the C 1*s* spectra obtained from regions 1–5, 6–10, and five regions outside the wear track, respectively.

were sampled in total and averaged to create the "outside" spectrum). The inset of Fig. 2(c) is a magnification of the C $1s \rightarrow \pi^*$ peaks for three spectra obtained by averaging the spectra from regions 1–5 (black line), 6–10 (gray line), and the regions outside the wear track (dotted line), respectively.

All spectra in Fig. 2(c) exhibit well-established and distinct spectral features associated with crystalline, sp^3-bonded carbon (diamond), including the sharp rise at the C $1s \rightarrow \sigma^*$ transition starting at 289 eV, the diamond exciton peak at 289.3 eV, and the second band gap dip at ~302 eV.[21] The peak at 285 eV is associated with sp^2-hybridized carbon and is due to the C $1s \rightarrow \pi^*$ transition in unsaturated carbon bonds. The sp^2-hybridized carbon in the grain boundaries of UNCD are the primary contributors to the peak at 285 eV.[6] Some additional contribution may come from adventitious carbon adsorbed from the atmosphere, and surface-reconstructed carbon bonds. The inset of Fig. 2(c) highlights the subtle differences in the carbon hybridization states between regions 1–5, 6–10, and outside the wear track. From these averaged data, the amount of sp^2 bonding as a fraction of all carbon bonds was determined to be slightly higher in regions 1–5 and regions 6–10 compared to outside the track, but the difference is small (<2% increase in each case). The slight increase in sp^2 bonding in the wear track compared to outside is attributed to a small number of tribochemical reactions that converted sp^3-bonded carbon to sp^2-bonded carbon.

A peak for the C $1s \rightarrow \pi^*$ transition of the C═O bond for nanocrystalline diamond is typically located within 286–287 eV,[22–24] and a peak for the C $1s \rightarrow \pi^*$ transition of the O═C–OH bond in carboxyl groups is typically located at ~288.7 eV.[22,25] The intensities of these peaks in the UNCD C 1*s* spectra are small and not significantly different between regions inside and outside the wear track. Thus, the UNCD film exhibits a small degree of oxidation that is independent of whether or not it has been exposed to wear. This oxidation is often seen on otherwise pristine films due to exposure to water and air. In addition, a subtle peak at 287.5 eV is present and is attributed to the C $1s \rightarrow \sigma^*$ transition of the C–H bond.[22] There is no observable change in the intensity of this peak between regions inside and outside the wear track. The small increase (<2%) in the amount of sp^2 bonding and the lack of oxidation and dehydrogenation in the wear track demonstrate the robustness of the UNCD film when subjected to wearing by a Si_3N_4 counterface in these experimental conditions.

The broad peaks observed in the O 1*s* XANES spectra (Fig. 3) at ~538 eV are due to the O $1s \rightarrow \sigma^*$ transition of the Si–O bond.[26] The peak for the O $1s \rightarrow \sigma^*$ transition for the C–O bond, if it were present, would be nearby at ~540 eV. The O 1*s* spectrum extracted from outside the wear track shows that the unworn UNCD film has very little oxygen, in agreement with the small C═O peak intensities in the C 1*s* spectra. The inset to Fig. 3 highlights the significant differences in average oxygen content between regions 1–5, 6–10, and outside the track. The averaged spectra from regions 1–5 show that overall these regions contain the highest amount of oxygen, which is in agreement with the contrast observed in the Si–O σ^* division map [Fig. 2(b)].

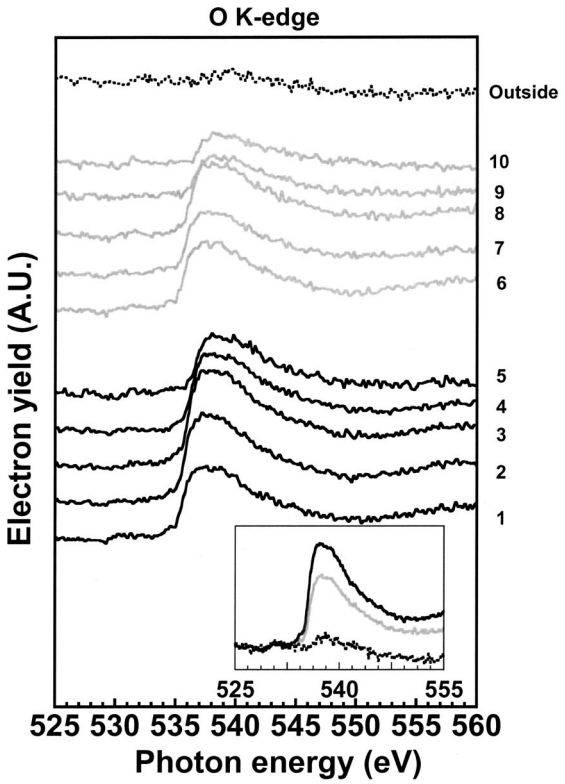

FIG. 3. O 1*s* XANES spectra obtained from the regions outlined in (b) and (c) of Fig. 2. The inset shows three average spectra obtained by averaging the O 1*s* spectra obtained from regions 1–5, 6–10, and five regions outside the wear track, respectively.

Figure 4 is a series of Si *L*-edge spectra. Spectra from regions 1–8 show similar spectroscopic features, namely, doublets with peaks at ~105.5 and ~106 eV, as well as broad peaks at ~108.5 eV. These are characteristic spectral features of silica tetrahedra (SiO_2).[26] The inset of Fig. 4 demonstrates that the average amount of silicon oxide is directly correlated with the average amount of oxygen (Fig. 3) in the wear track. This indicates that the increased amount of oxygen (above the "background" amount intrinsic to the UNCD film) present within the wear track is oxygen from the silica and not from C–O bonding. These results provide evidence that the Si_3N_4 ball is worn by the UNCD surface, and this results in the deposition of silica into the wear track. N 1*s* spectra were also extracted from inside and outside the wear track, but no evidence of nitrogen was found. These results are consistent with the findings of Tomizawa and Fischer[27] from their study of self-mated Si_3N_4 interfaces in a humid environment, whereby they discovered silicon oxide tribochemical reaction products on the wear tracks.

The Raman spectra [Fig. 5(a)] and corresponding optical micrograph [Fig. 5(b)] taken on the Si_3N_4 ball show that the worn region of the ball is spectroscopically and morphologically distinct from its unworn areas. Specifically, two peaks in the Raman spectrum taken on the worn region of the ball are not observed elsewhere. The two broad Raman features

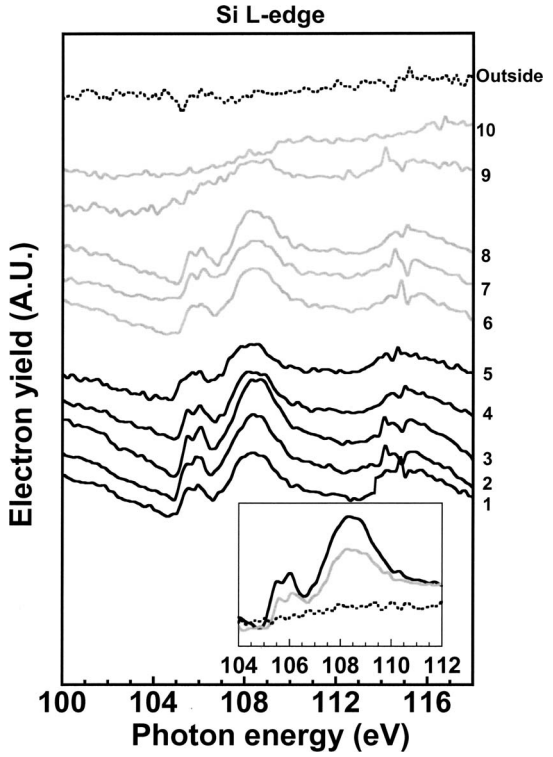

FIG. 4. Si *L*-edge XANES spectra obtained from the regions outlined in (b) and (c) of Fig. 2. (inset) Three average spectra obtained by averaging the Si *L*-edge spectra obtained from regions 1–5, 6–10, and five regions outside the wear track, respectively.

at ~1346 and ~1595 cm^{-1} are the *D* and *G* peaks, respectively, characteristic of disordered sp^2-bonded carbon.[28] This suggests that some amount of carbon from the sample underwent a tribochemically induced conversion from $sp^3 \rightarrow sp^2$ bonding and was transferred to the Si_3N_4 ball in the form of disordered carbon, often seen with diamondlike carbon (DLC)-type coatings.[4,29]

IV. CONCLUSIONS

By using the X-PEEM technique, we were able to draw definitive conclusions about the composition and bonding of the atoms in a UNCD wear track. The results show that sliding a Si_3N_4 ball across the surface of UNCD results in the deposition of silica in the wear track, but the bonding structure of UNCD in the wear track is not significantly modified by tribomechanical wear. Only a small amount of sp^3-hybridized carbon bonds are converted into sp^2-hybridized carbon bonds. Raman spectroscopy showed that disordered carbon was present on the surface of the Si_3N_4 ball. This demonstrates that the remaining UNCD film remained predominantly in its original form, with some silica deposited on top of it. As well, some amount of carbon was removed from the UNCD surface and accumulated onto the ball in a disordered sp^2 bonding configuration.

The advanced methods employed for this study can be used to analyze a wide range of materials, including candidate materials for MEMS/NEMS systems involving contacting and/or sliding components. Because of the important but complex role that tribochemistry, transfer films, and third bodies play in dictating the behavior of materials in tribological contact, this type of experimental approach can help reveal in detail the mechanisms at play in a tribological interface.

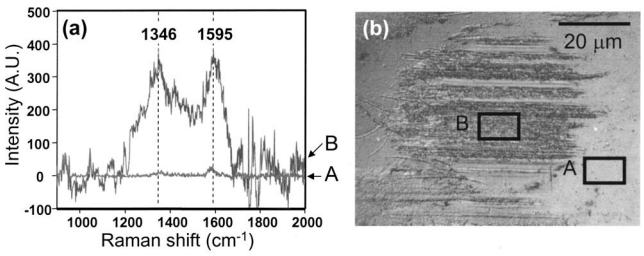

FIG. 5. (a) Raman spectra taken from the worn and unworn regions of the Si_3N_4 ball and (b) corresponding optical image of the ball.

ACKNOWLEDGMENTS

Funding was provided by Air Force Grant No. FA9550-05-1-0204 to RWC and PUPAG. Additional funding for the X-PEEM experiments was provided by the NSF Grant Nos. CHE-0613972, PHY-0523905, and PHY-0646018 to PUPAG. All X-PEEM experiments were performed at the UW-SRC, a national facility supported by the NSF under Award No. DMR-0537588. Work at Argonne was supported by the U.S. Department of Energy, BES-Materials Sciences, under Contract No. DE-AC02-06CH11357. Sandia is a multiprogram laboratory operated by Sandia Corporation, a Lockheed Martin Company for the United States Department of Energy under Contract No. DE-AC04-94AL8500. The authors thank David Tallant and Gina Simpson for micro-Raman measurements.

[1]T. E. Fischer, Annu. Rev. Mater. Sci. **18**, 303 (1988).
[2]M. Godet, Wear **100**, 437 (1984).
[3]I. L. Singer, Langmuir **12**, 4486 (1996).
[4]I. L. Singer, S. D. Dvorak, K. J. Wahl, and T. W. Scharf, J. Vac. Sci. Technol. A **21**, 232 (2003).
[5]R. F. Davis, *Diamond Films and Coatings* (Noyes, Park Ridge, NJ, 1992).
[6]D. M. Gruen *et al.*, Appl. Phys. Lett. **68**, 1640 (1996).
[7]N. N. Naguib *et al.*, Chem. Phys. Lett. **430**, 345 (2006).
[8]H. D. Espinosa and B. Peng, J. Microelectromech. Syst. **14**, 153 (2005).
[9]H. D. Espinosa, B. Peng, B. C. Prorok, N. Moldovan, O. Auciello, J. A. Carlisle, D. M. Gruen, and D. C. Mancini, J. Appl. Phys. **94**, 6076 (2003).
[10]A. R. Krauss *et al.*, Diamond Relat. Mater. **10**, 1952 (2001).
[11]A. V. Sumant *et al.*, Mater. Res. Soc. Symp. Proc. **657**, 5 (2001).
[12]B. H. Frazer, M. Girasole, L. M. Wiese, T. Franz, and G. D. Stasio, Ultramicroscopy **99**, 87 (2004).
[13]B. H. Frazer, B. Gilbert, B. R. Sonderegger, and G. De Stasio, Surf. Sci. **537**, 161 (2003).
[14]G. W. Canning, M. L. Suominen Fuller, G. M. Bancroft, M. Kasrai, J. N. Cutler, G. De Stasio, and B. Gilbert, Tribol. Lett. **6**, 159 (1999).
[15]M. A. Nicholls, G. M. Bancroft, M. Kasrai, P. R. Norton, B. H. Frazer, and G. De Stasio, Tribol. Lett. **18**, 453 (2005).
[16]S. Anders, T. Stammler, W. Fong, D. B. Bogy, C. S. Bhatia, and J. Stöhr, J. Vac. Sci. Technol. A **17**, 2731 (1999).
[17]C. S. Bhatia, F. Walton, C. Chao-Yuan, W. Jianjun, D. B. Bogy, S. Anders, T. Stammler, and J. Stöhr, IEEE Trans. Magn. **35**, 910 (1999).
[18]S. Anders, T. Stammler, W. Fong, C. Chao-Yuan, D. B. Bogy, C. S. Bhatia, and J. Stöhr, J. Tribol. **121**, 961 (1999).
[19]A. Erdemir, M. Halter, G. R. Fenske, C. Zuiker, R. Csencsits, A. R.

Krauss, and D. M. Gruen, Tribol. Trans. **40**, 667 (1997).
[20]A. Erdemir, G. R. Fenske, A. R. Krauss, D. M. Gruen, T. McCauley, and R. T. Csencsits, Surf. Coat. Technol. **120–121**, 565 (1999).
[21]F. L. Coffman, R. Cao, P. A. Pianetta, S. Kapoor, M. Kelly, and L. J. Terminello, Appl. Phys. Lett. **69**, 568 (1996).
[22]J. Stöhr, *NEXAFS Spectroscopy* (Springer, Berlin, Heidelberg, 1992).
[23]S. Osswald, G. Yushin, V. Mochalin, S. O. Kucheyev, and Y. Gogotsi, J. Am. Chem. Soc. **128**, 11635 (2006).
[24]M. Jaouen, G. Tourillon, J. Delafond, N. Junqua, and G. Hug, Diamond Relat. Mater. **4**, 200 (1995).
[25]J. Diaz, S. Anders, A. Cossy-Favre, M. Samant, and J. Stöhr, J. Vac. Sci. Technol. A **17**, 2737 (1999).
[26]B. Gilbert, B. H. Frazer, F. Naab, J. Fournelle, J. W. Valley, and G. De Stasio, Am. Mineral. **88**, 763 (2003).
[27]H. Tomizawa and T. E. Fischer, ASLE Trans. **29**, 481 (1986).
[28]D. S. Knight and W. B. White, J. Mater. Res. **4**, 385 (1989).
[29]Y. Liu, A. Erdemir, and E. I. Meletis, Surf. Coat. Technol. **86–87**, 564 (1996).